



DYNAMIC ANALYSIS OF A TALL BUILDING WITH A TUNED-MASS-DAMPER DEVICE SUBJECTED TO EARTHQUAKE EXCITATIONS

A.-P. WANG

Department of Civil Engineering, Chung Yuan Christian University, Chung-Li, Taiwan 32023, R.O.C.

R.-F. FUNG

*Department of Mechanical and Automation Engineering, National Kaohsiung First University of Science
and Technology, University Road, Yuanchau, Kaohsiung 824, Taiwan, R.O.C.*

E-mail: rffung@ccms.nkfust.edu.tw

AND

S.-C. HUANG

*Department of Mechanical Engineering, Chung Yuan Christian University, Chung-Li,
Taiwan 32023, R.O.C.*

(Received 31 May 2000, and in final form 23 October 2000)

In this paper, Hamilton's principle and finite element method are employed to formulate the new dynamic equation of a tall building subjected to earthquake excitations. A tuned-mass-damper (TMD) system is installed at the top to absorb the earthquake-induced vibrations. First, the non-linear governing equations in the axial and transverse directions are obtained by the Euler-beam theory. Secondly, the simple-flexure beam model is employed to reduce the system as a linear one. The energetic analyses of these two beam theories are provided. It is found that the rigid-body motion of the TMD and the transversal vibrations of the tall building are coupled and energy is transferred between them. Finally, the effects of several parameters on the rigid-body motion and transversal vibrations are presented and discussed.

© 2001 Academic Press

1. INTRODUCTION

In recent years, more and more of supertall constructions have been built. While the top of a building is over and above some degree, the dynamic behavior of this building is parallel to a beam with several lumped masses. The vibration problems of high-rise tall buildings subjected to certain dynamic loadings, such as earthquake loads or wind loads, have attracted the interest of investigations in this area. The finite element method and Hamilton's principle were usually used to formulate and analyze the dynamic behavior of tall buildings. The earlier studies [1, 2] recommended that for increasing the levels of structural safety, integrity and occupant comfort, it is necessary to reduce the levels of earthquake- or wind-induced displacements and accelerations in tall buildings.

As a result, various control schemes—passive as well as active—have been developed to reduce the building vibrations due to these environmental disturbances. One of the earlier investigations in the application of theoretical control methods to civil engineering

structures was reported by Yang [3], in which the optimal control strategies were used for tall buildings, which were modelled as shear beams and subjected to wind loads. In another noteworthy study [4], stochastic wind model was employed to examine the performance of the tuned passive vibration absorbers to damp out excessive vibration levels. The active control of tall buildings using aerodynamic appendages has been of interest to several researchers [5–7] because the energy needed to generate the control force is provided by the wind.

In this paper, the model of a tall building is considered as a continuum that is different from the previous studies [1–8] of the lumped parameter system. In fact, the civil structure in itself is a continuum having infinite degrees of freedom and comprising several concentrated masses. In this paper, the non-linear Euler-beam theory and the simple-flexure beam model are employed to model a tall building with many masses of floors and a TMD installed at its top. First, the transversal vibrations of the tall building coupled with the rigid-body motion of the TMD are formulated by Hamilton's principle. The TMD is designed to absorb the transversal vibrations of the tall building. It is found that the dynamic responses of the tall building are effectively reduced when the TMD frequency is tuned to be the same as that of the building. Secondly, the whole system is formulated by the finite element method. Some observations from the coupled governing equations and boundary conditions are made. Finally, numerical results via the finite element method are compared for the linear and non-linear systems.

2. DYNAMIC FORMULATION

A schematic drawing of an n -story-building model subjected to earthquake motion $b(t)$ and a TMD system installed at its top floor is shown in Figure 1(a). The tall building is modelled by the elastic beam theory with uniform flexibility. The n concentrated masses m_i are located at x_i , $i = 1, 2, \dots, n$ respectively. The TMD is a passive energy-absorbing system and is shown in Figure 1(b), which consists of a mass M_G , and a spring with a constant stiffness k . The purpose of this device is to absorb the earthquake-induced vibrations of the tall building. It is assumed that the contact surface between the tuned mass M_G and the top floor m_n is dry. The friction force opposing their relative motion is called Coulomb damping and its magnitude is denoted by $\mu M_G g$, in which μ is the so-called kinetic coefficient of friction.

2.1. KINETIC AND POTENTIAL ENERGIES

Since the tall building is subjected to earthquake, the fixed (OXY) and moving (oxy) co-ordinates are adopted to describe the whole system. The tall building has length ℓ density ρ , uniform cross-sectional area A , modulus of elasticity E , and moment of inertia I . In Figure 1(b), ξ is the displacement of mass M_G relative to the n th floor.

The displacement field of the tall building modelled by the Euler-beam theory is

$$\mathbf{r} = u(x, t)\mathbf{i} + v(x, t)\mathbf{j}, \quad (1)$$

where $u(x, t)$ and $v(x, t)$ represent the axial and transverse deflections respectively. \mathbf{i} and \mathbf{j} are the unit vectors of the moving co-ordinate (oxy). The position vector of an arbitrary point after deformation is

$$\mathbf{R} = [x + u(x, t)]\mathbf{i} + [v(x, t) + b(t)]\mathbf{j}. \quad (2)$$

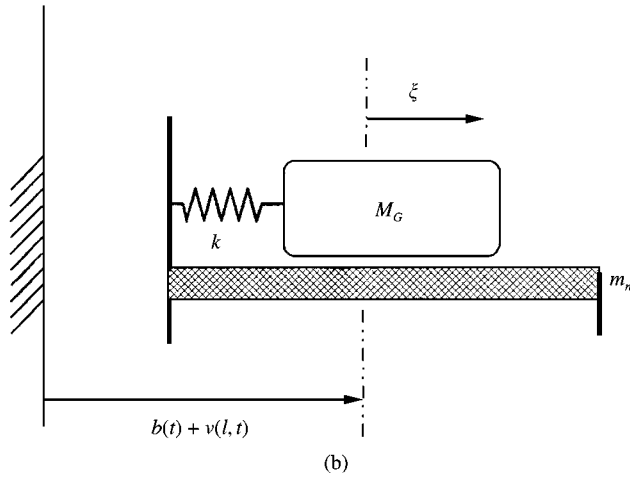
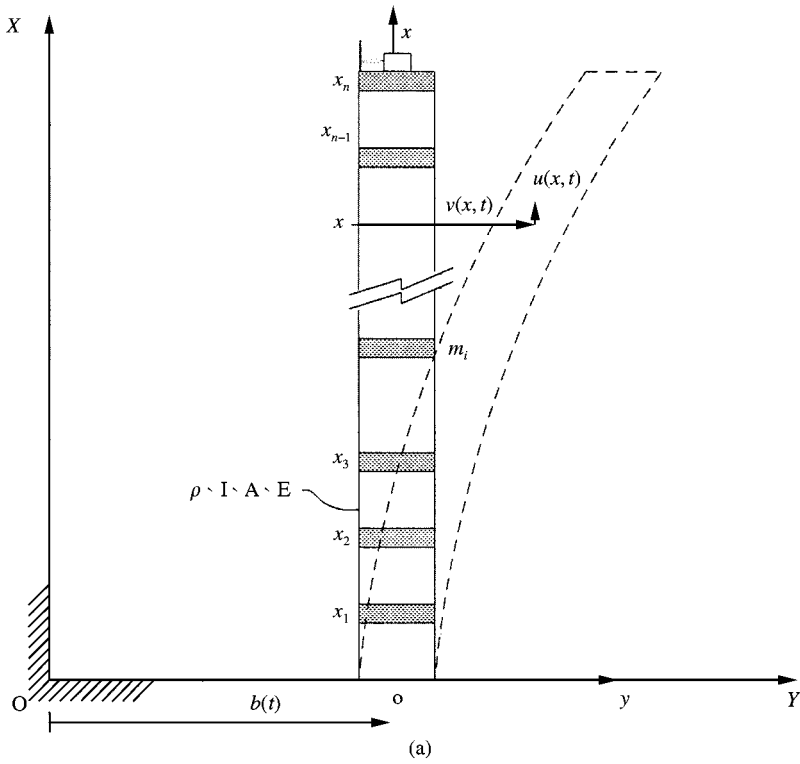


Figure 1. Schematic diagrams. (a) The tall building with the TMD system; (b) the TMD device.

Therefore, the total kinetic energy of the whole system including a uniform beam, n floors and the TMD device is

$$\begin{aligned}
 T = & \int_0^{\ell} \frac{1}{2} \rho A \{ \dot{u}^2 + (\dot{v} + \dot{b})^2 \} dx + \int_0^{\ell} \sum_{i=1}^n \frac{1}{2} m_i \{ \dot{u}^2 + (\dot{v} + \dot{b})^2 \} \delta(x - x_i) dx \\
 & + \frac{1}{2} M_G \{ \dot{u}^2(\ell, t) + [\dot{v}(\ell, t) + \dot{b} + \dot{\xi}]^2 \}.
 \end{aligned} \tag{3}$$

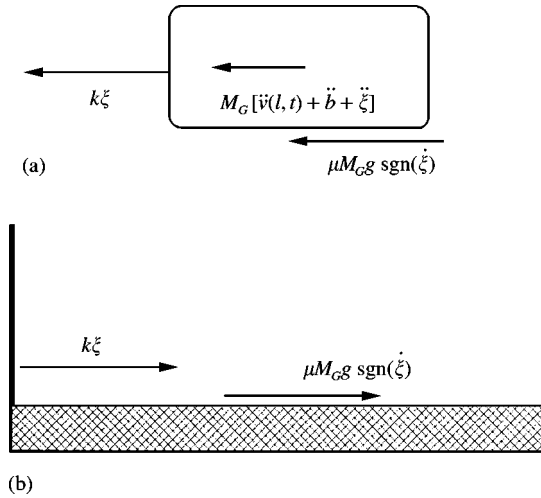


Figure 2. Free-body diagrams. (a) The TMD system; (b) the top floor.

It is assumed in equation (3) that the center distance between the tuned mass M_G and the n th floor is too small compared with the beam length ℓ . Thus, the location of mass M_G is regarded to be at $x = \ell$.

The Lagrangian strains of the tall building in the corresponding directions are

$$\epsilon_{xx} = u_x - yv_{xx} + \frac{1}{2}v_x^2, \quad \epsilon_{xy} = 0, \quad \epsilon_{yy} = 0, \quad (4-6)$$

where the subscript x is defined as partial derivative with respect to x . The non-linear term $\frac{1}{2}v_x^2$ due to large geometric deformation in the transverse direction is considered. The total potential energy can be written as

$$U = \int_0^\ell \frac{1}{2} \left[EA \left(u_x^2 + \frac{1}{4}v_x^4 + u_x v_x^2 \right) + EI v_{xx}^2 \right] dx - \int_0^\ell G(x) u_x dx + \frac{1}{2} k \xi^2, \quad (7)$$

where

$$G(x) = -g \left[\rho A (\ell - x) + \sum_{i=1}^n m_i H(x_i - x) + M_G \right] \quad (8)$$

is the gravitational force due to the distributed beam, n floors and the tuned mass M_G . H is the unit step function.

The free-body diagrams of the tuned mass M_G and the top floor are shown in Figures 2(a) and (b) respectively. The sign function is defined as

$$\text{sgn}(\dot{\xi}) = \begin{cases} +1, & \dot{\xi} > 0 \\ -1, & \dot{\xi} < 0 \end{cases}$$

In addition, the virtual work done by the non-conservative friction force between the n th floor and the tuned mass, associated with a virtual displacement $\delta v(\ell, t)$, is

$$\delta W = -\mu M_G g \text{sgn}(\dot{\xi}) \delta \xi. \quad (9)$$

2.2. THE EULER-BEAM THEORY

Substituting equations (3), (7) and (9) into Hamilton's principle

$$\int_{t_1}^{t_2} [\delta(T - U) + \delta W] dt = 0, \quad (10)$$

taking variation, applying integration by parts, and collecting the like terms, one obtains the governing equations for the axial and transversal vibrations of the tall building, and the rigid-body motion of the tuned mass respectively:

$$u \quad \rho A \ddot{u} + \sum_{i=1}^{n-1} m_i \ddot{u} \delta(x - x_i) - EA \frac{\partial}{\partial x} \left[u_x + \frac{1}{2} v_x^2 \right] + \frac{\partial}{\partial x} [G(x)] = 0, \quad 0 < x < \ell \quad (11)$$

$$v \quad \rho A (\ddot{v} + \ddot{b}) + \sum_{i=1}^{n-1} m_i (\ddot{v} + \ddot{b}) \delta(x - x_i) + EI v_{xxxx} - EA \frac{\partial}{\partial x} \left[\frac{1}{2} v_x^3 + u_x v_x \right] = 0, \quad 0 < x < \ell \quad (12)$$

$$\xi \quad M_G [\ddot{v}(\ell, t) + \ddot{b} + \ddot{\xi}] + k\xi + \mu M_G g \operatorname{sgn}(\dot{\xi}) = 0, \quad (13)$$

and the associated boundary conditions:

$$u(0, t) = 0, \quad v(0, t) = 0, \quad v_x(0, t) = 0. \quad (14-16)$$

$$u(\ell, t) \quad (M_G + m_n) \ddot{u}(\ell, t) + EA [u_x(\ell, t) + \frac{1}{2} v_x^2(\ell, t)] + (M_G + m_n)g = 0, \quad (17)$$

$$v(\ell, t) \quad M_G [\ddot{v}(\ell, t) + \ddot{b} + \ddot{\xi}] + m_n [\ddot{v}(\ell, t) + \ddot{b}] \\ + EA \left[\frac{1}{2} v_x^3(\ell, t) + u_x(\ell, t) v_x(\ell, t) \right] - EI v_{xxx}(\ell, t) = 0, \quad (18)$$

$$v_{xx}(\ell, t) = 0, \quad (19)$$

where δ is the Dirac-delta function. It can be observed that (1) the acceleration \ddot{b} of earthquake motion appears in the transverse vibration equation (12) and its boundary condition (18), (2) the axial and transverse vibrations are non-linearly coupled in the governing equations (11) and (12) and boundary conditions (17) and (18), and (3) equation (18) states the force equilibrium in the transverse direction at $x = \ell$, and the free-body diagram is shown in Figure 2(b). Equation (18) can be rewritten together with equation (13) as

$$EA \left[\frac{1}{2} v_x^3(\ell, t) + u_x(\ell, t) v_x(\ell, t) \right] - EI v_{xxx}(\ell, t) + k\xi + \mu M_G g \operatorname{sgn}(\dot{\xi}) = 0. \quad (20)$$

2.3. THE SIMPLE-FLEXURE BEAM MODEL

The simple-flexure beam model [9] is the Euler-beam theory with quasi-static stretching assumption, in which one will eliminate the axial inertia effect. The reduction process is to incorporate these effects of equation (11) into equation (12). Thus, one may define the internal axial force as

$$p(x, t) = EA [u_x(x, t) + \frac{1}{2} v_x^2(x, t)]. \quad (21)$$

By taking $x = \ell$ in equation (21) and using equation (17), the relationship between the internal force at $x = \ell$ and the external force is

$$p(\ell, t) = EA[u_x(\ell, t) + \frac{1}{2}v_x^2(\ell, t)] = G(x). \quad (22)$$

As a result, we have

$$p(x, t) = p(\ell, t) - \int_x^\ell \frac{\partial}{\partial x} p(x, t) dx = -g \left[M_G + \rho A(\ell - x) + \sum_{i=1}^n m_i H(x_i - x) \right], \quad (23)$$

in which the inertial terms of equation (11) are neglected for the simple-flexure beam model. Alternatively, formula (23) can be obtained directly from equation (11) by neglecting the inertia effects [10].

Consequently, the governing equations (11)–(13) can be reduced to two equations:

$$\rho A(\ddot{v} + \ddot{b}) + \sum_{i=1}^n m_i(\ddot{v} + \ddot{b})\delta(x - x_i) + EIV_{xxx} - G(x)v_{xx} - \rho Agv_x = 0, \quad 0 < x < \ell, \quad (24)$$

$$M_G[\ddot{v}(\ell, t) + \ddot{b} + \ddot{\xi}] + k\xi + \mu M_G g \operatorname{sgn}(\dot{\xi}) = 0, \quad (25)$$

and the boundary conditions are

$$v(0, t) = 0, \quad v_x(0, t) = 0, \quad (26, 27)$$

$$M_G[\ddot{v}(\ell, t) + \ddot{b} + \ddot{\xi}] + m_n[\ddot{v}(\ell, t) + \ddot{b}] - EIV_{xxx}(\ell, t) - g(M_G + m_n)v_x(\ell, t) = 0, \quad (28)$$

$$v_{xx}(\ell, t) = 0. \quad (29)$$

It is seen that the effects of axial displacement and non-linear term disappear in governing equation (24) and boundary condition (28).

Governing equations (24) and (25) and boundary conditions (26)–(29) can also be obtained directly by Hamilton's principle with the following kinetic energy and strain energy:

$$T = \int_0^\ell \frac{1}{2} \rho A(\dot{v} + \dot{b})^2 dx + \int_0^\ell \sum_{i=1}^n \left[\frac{1}{2} m_i(\dot{v} + \dot{b})^2 \delta(x - x_i) \right] dx + \frac{1}{2} M_G[\dot{v}(\ell, t) + \dot{b} + \dot{\xi}]^2, \quad (30)$$

$$U = \int_0^\ell \frac{1}{2} (EIV_{xx}^2) dx + \int_0^\ell \frac{1}{2} G(x)v_x^2 dx + \frac{1}{2} k\xi^2, \quad (31)$$

where $G(x)$ is the same as in equation (8). In Hamilton's principle, the virtual work is also the same as in equation (9).

2.4. RIGID-BODY MODEL

The governing equation for the rigid-body building, i.e., neglecting all the flexible terms, is

$$M_G(\ddot{b} + \ddot{\xi}) + k\xi + \mu M_G g \operatorname{sgn}(\dot{\xi}) = F. \quad (32)$$

It is the governing equation for the TMD device subjected to earthquake excitations.

2.5. DISCUSSION

One main objective of this paper is to formulate the new dynamic equations of a continuous tall building with the TMD device. The reduction process was done by starting with the Euler-beam theory and going through the simple-flexure beam model, and finally the rigid-body model. From the dynamic formulations of the governing equations and boundary conditions, several important observations can be made. (1) In the simple-flexure beam model, the $v(x, t)$ governing equation (24) becomes linear. Boundary condition (28) representing the shear force balancing at the top floor couples with the motion of the tuned mass. (2) The transversal vibrations of the flexible building and the rigid-body motion of the TMD are coupled in both the Euler-beam theory and the simple-flexure beam model. Thus, a complete formulation of the continuous tall building with the TMD device should include both the rigid-body motion and transversal vibrations.

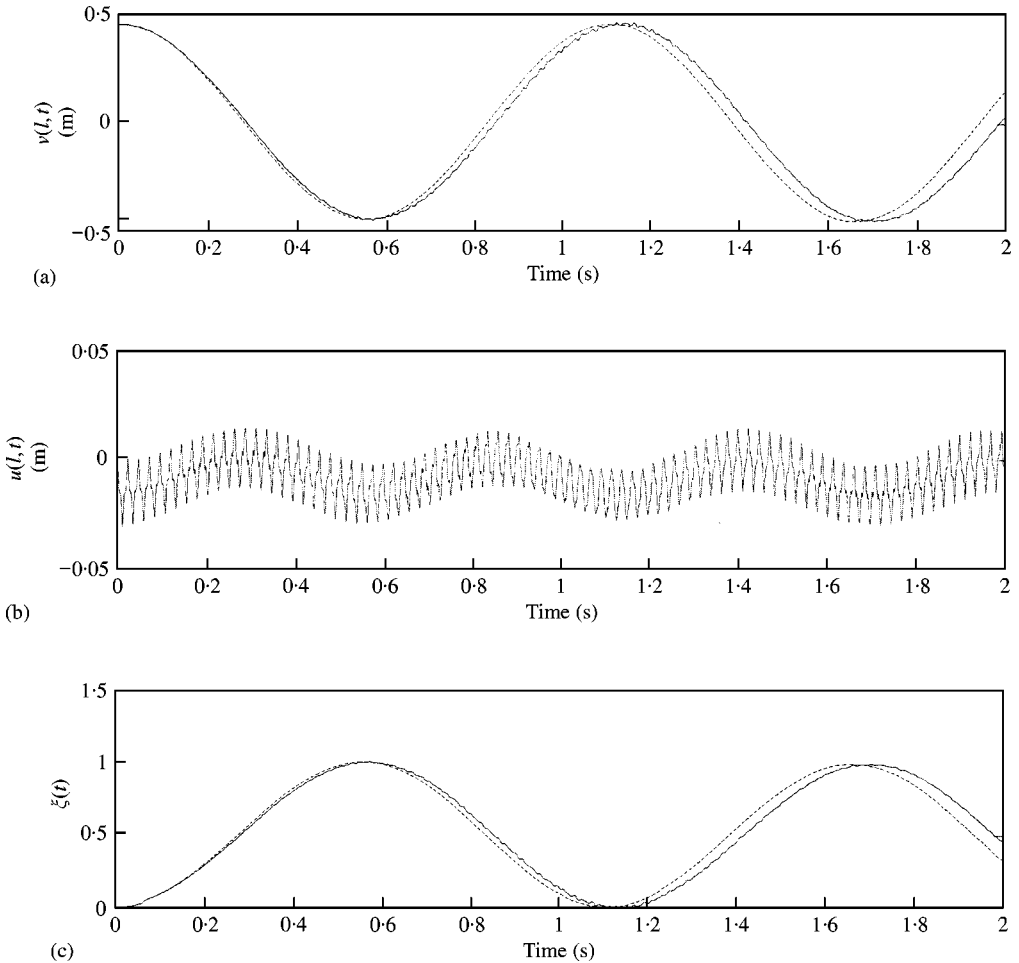


Figure 3. The transient response diagrams. (a) The top-floor displacements in the transverse direction; (b) the top-floor displacements in the longitudinal direction; (c) the tuned-mass displacements: —, the non-linear Euler-beam theory; ---, the simple-flexure beam model.

3. NUMERICAL RESULTS

In this paper, the Euler-beam theory and the simple-flexure beam model are both studied by the finite element formulation, in which the continuous displacements are approximated in terms of the discretized nodal displacements. The flexible beam is divided into n elements. The detailed finite element formulation can be seen in Appendix A.

In order to speed-up the computational simulation, a three-floor building is given as an example for dynamic analysis. The parameters of the tall building and the TMD device are selected as $\ell = 9$ m, $E = 2.1324 \times 10^{10}$ N/m², $A = 0.075$ m², $I = 5.625 \times 10^{-4}$ m⁴, $\rho = 7840$ kg/m³, $M_G = 91.95$ kg, and each floor mass $m_i = 194.25$ kg.

First, we show the transient free responses of the top floor and the TMD for the given parameters $\mu = 0$, $k = 0$ N/m and $F = 0$. The first-mode shape of the uniform beam is adopted for the initial displacement:

$$v(x, 0) = C[\sin(\beta x) - \sinh(\beta x) - \alpha(\cos(\beta x) - \cosh(\beta x))], \quad (33)$$

where $\beta\ell = 1.875104$, $\alpha = ((\sin(\beta\ell) + \sinh(\beta\ell))/(\cos(\beta\ell) + \cosh(\beta\ell)))$, and the coefficient $C = 0.1835$ is assigned. The other initial displacements are zero.

The transverse and longitudinal responses of the non-linear Euler-beam theory and the simple-flexure beam model are compared in Figures 3(a)–(c). It can be examined that the oscillational periods of the building and the tuned mass are almost the same as $(2\pi\beta^2)\rho A/EI = 1.0135$ (s) which is the first-mode period of a uniform cantilever beam without the lumped masses of floors. The non-linear terms have the effects of increasing the transverse oscillation periods [Figure 3(a)] and increasing the amplitude in the longitudinal direction [Figure 3(b)]. The longitudinal displacements are much smaller than those in the transverse direction. Thus, the two-dimensional formulation can be simplified as a one-dimensional problem. Since the energy could transfer from the building to the TMD, it

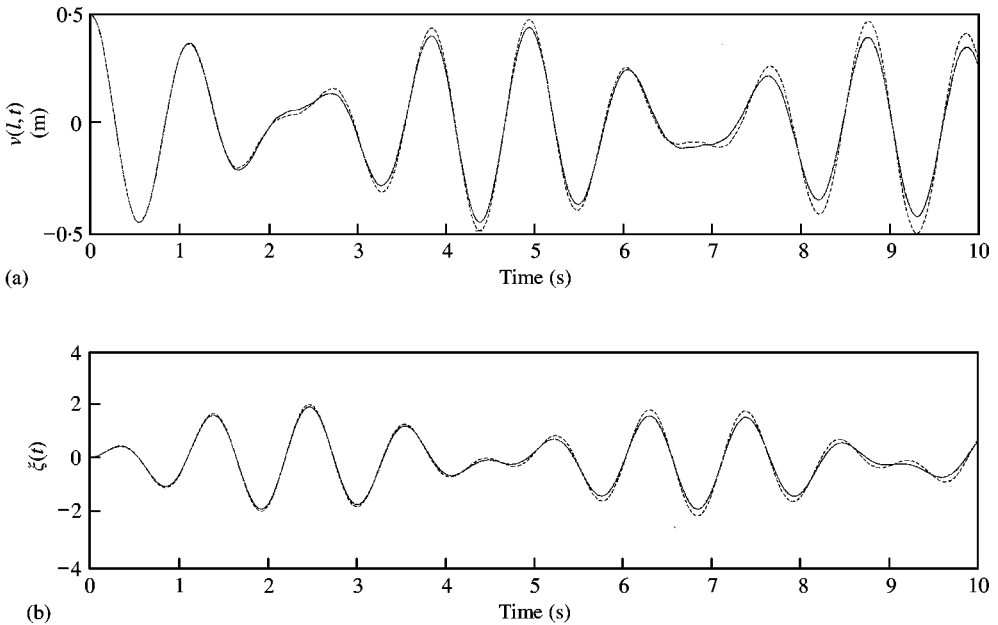


Figure 4. The passive-control responses subjected to an initial displacement. (a) The top-floor vibration; (b) the TMD vibration: —, $\mu = 0.05$; - - -, $\mu = 0$.

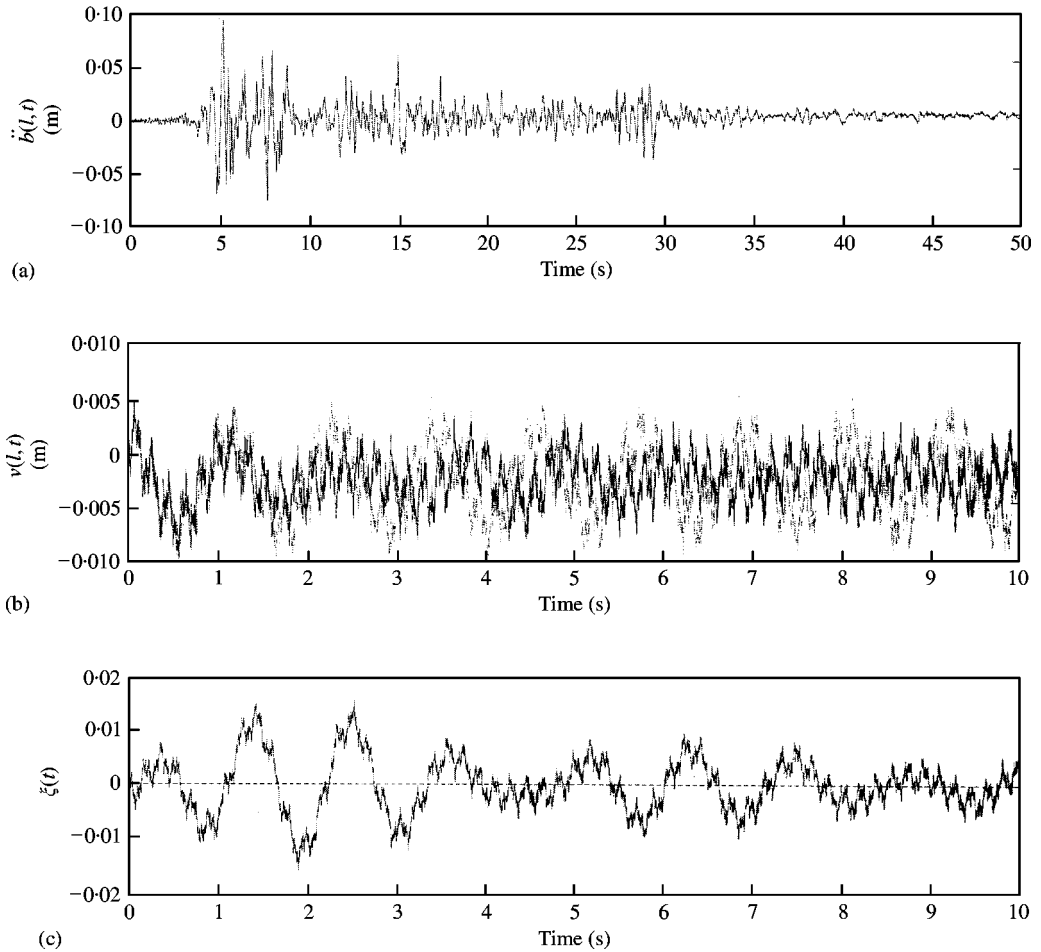


Figure 5. The passive-control responses subjected to the El Centro earthquake. (a) The acceleration of the El Centro earthquake; (b) the displacements of the top floor; (c) the displacements of the TMD: —, $\mu = 0.05$; \cdots , without the passive control.

is observed in Figures 3(a) and (c) that the maximum moving distance of the tuned mass is about two times the maximum displacement of the top floor.

In this paper, we are only interested in the passive control of the tall building with the TMD device subjected to the initial displacement and earthquake excitations. The results are shown in Figures 4–6. The spring stiffness k of the TMD device is adjusted so that the natural frequency of the TMD equals the first-mode frequency of the building. In this case, the spring stiffness is $k = 3011.67$ N/m. Then, the TMD becomes a passive-control device to absorb the first-mode vibrations of the building. Figure 4 shows the passive control responses due to an initial displacement. In fact, the frequency of the TMD is close to, but not exactly equal to, the natural frequency of the building, the beating phenomenon occurs in the simulation results. It is seen that as the dry friction is introduced, the vibration suppression is more effective. Figures 5(a) and 6(a) show the seismic accelerations of the El Centro and Kobe earthquakes respectively. In order to save computational time, the transient responses within 10 s are shown. The vibrations of the tall building are passively controlled and are shown in Figures 5(b) and 6(b). The displacements of the TMD are shown in Figures 5(c) and 6(c).

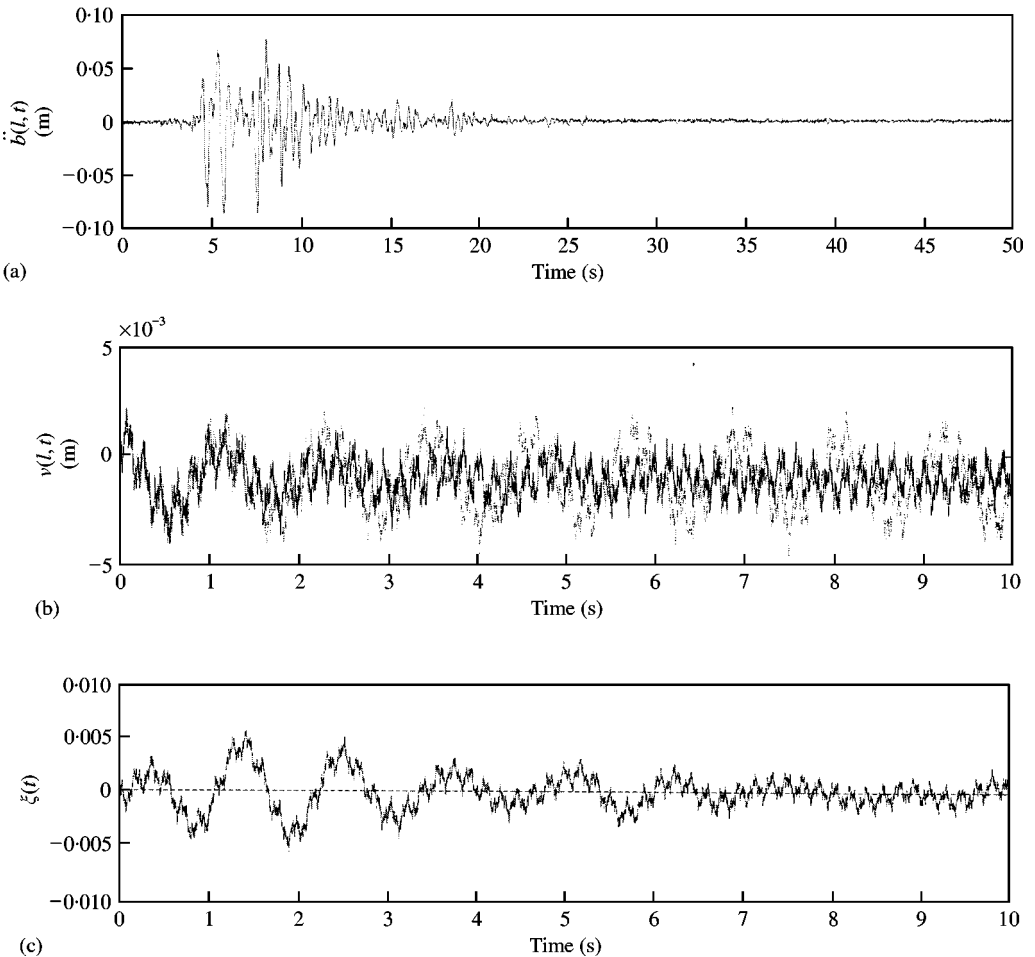


Figure 6. The passive-control responses subjected to the Kobe earthquake. (a) The acceleration of the Kobe earthquake; (b) the displacements of the top floor; (c) the displacements of the TMD: —, $\mu = 0.05$; ···, without the passive control.

4. CONCLUSIONS

The transversal vibrations of a continuous tall building coupled with the rigid-body motion of the TMD device are successfully formulated via Hamilton's principle in this paper. From the dynamic formulations and numerical results, the following conclusions can be drawn.

- (1) For the tall building system, a two-dimensional problem can be reduced to a one-dimensional one via the simple-flexure beam model.
- (2) The rigid-body motion and transversal vibrations are always coupled in both the Euler-beam theory and the simple-flexure beam model. A complete analysis of the tall building associated with the TMD device should include both the rigid-body motion and transversal vibrations.
- (3) The gravitational forces due to the floor masses and the TMD device appear in both the Euler-beam theory and the simple-flexure beam model.

- (4) The displacement of the tuned mass is much larger than that of the top floor. It is found that the TMD needs more space to operate in real application.

ACKNOWLEDGMENTS

Support of this work by the National Science Council of the Republic of China Contract NSC-88-2212-E033-002 is gratefully acknowledged.

REFERENCES

1. F.-K. CHANG 1973 *American Society of Civil Engineers, Journal of The Structure Division* **99**, 1259–1272. Human response to motions in tall buildings.
2. R. J. HANSEN, J. W. REED and E. H. VANMARCKE 1973 *American Society of Civil Engineers, Journal of The Structure Division* **99**, 1589–1605. Human response to wind-induced motion of the buildings.
3. J. N. YANG 1995 *American Society of Civil Engineers, Journal of Engineering Mechanics* **101**, 819–838. Application of optimal control theory to civil engineering structures.
4. R. J. MCNAMARA 1977 *American Society of Civil Engineers, Journal of The Structure Division* **103**, 100–200. Tuned mass dampers for buildings.
5. R. E. KLEIN, C. CUSANO and J. U. SLUKEL 1972 Paper No. 72-W +/AIT-11. Presented at the ASME Winter Annual Meeting, 1972 New York, NY. Investigation of method to stabilize wind induced oscillations in large structures.
6. J. C. CHANG and T. T. SOONG 1980 *Structural Control* (H. Leipholz, editor) 199–120. IUTAM, New York, NY: North-Holland Publishing Co. and SM Publications. The use of aerodynamic appendages for tall building control.
7. T. T. SOONG and G. T. SKINNER 1981 *American Society of Civil Engineers, Journal of Engineering Mechanics* **107**, 1057–1068. Experimental study of active structural control.
8. A. OHSUMI and Y. SAWADA 1993 *American Society of Mechanical Engineers, Journal of Dynamic Systems, Measurement, and Control* **115**, 649–657. Active control of flexible structures subject to distributed and seismic disturbances.
9. R. F. FUNG and H. C. CHANG 1998 *Journal of Sound and Vibration* **216**, 751–769. Dynamic modeling of a non-linearly constrained flexible manipulator with a tip mass by Hamilton's principle.
10. R. LEWANDOWSKI 1987 *Journal of Sound and Vibration*, **114**, 91–101. Application of the Ritz method to the analysis of non-linear free vibrations of beams.
11. C. C. SPYRAKOS 1994 *Finite Element Modeling in Engineering Practice*. Morgantown, WV: West Virginia University Press.
12. J. N. REDDY 1993 *An Introduction to The Finite Element Method*. New York: McGraw-Hill, Inc.

APPENDIX A

The usual approach in the finite element method is to assume the unknown deformations $u(x, t)$ and $v(x, t)$ to be approximated by a finite series:

$$u(x, t) = \sum_{i=1}^n H_{ui}(x)q_i(t), \quad (\text{A1})$$

$$v(x, t) = \sum_{i=1}^n H_{vi}(x)q_i(t), \quad (\text{A2})$$

where $H_{ui}(x)$ and $H_{vi}(x)$ are the Hermite shape functions [11]:

$$H_{ui}(x) = a_{ui} + b_{ui}x, \quad i = 1, 2, \quad (\text{A3})$$

$$H_{vi}(x) = a_{vi} + b_{vi}x + c_{vi}x^2 + d_{vi}x^3, \quad i = 1-4. \quad (\text{A4})$$

The displacement shape function (A3) has two degrees of freedom. There is an axial displacement at each node. The complete cubic polynomial function (A4) has four degrees of freedom (a transverse displacement and a small rotation at each node) for an element. The shape functions \mathbf{H}_u and \mathbf{H}_v of a beam element can be found as

$$\mathbf{H}_u = \begin{bmatrix} 1 - \frac{x}{\ell} \\ \frac{x}{\ell} \end{bmatrix}, \quad (\text{A5})$$

$$\mathbf{H}_v = \frac{1}{\ell^3} [2x^3 - 3x^3\ell + \ell^3 \quad x^3 - 2x^2\ell + x\ell^2 \quad -2x^3 + 3x^2\ell \quad x^3\ell - x^2\ell^2], \quad (\text{A6})$$

and the nodal displacement vector \mathbf{q} can be written as

$$\mathbf{q} = [q_1 \quad q_2 \quad q_3 \quad q_4 \quad q_5 \quad q_6]^T. \quad (\text{A7})$$

A.1. THE NON-LINEAR EULER-BEAM THEORY

Substituting equations (A1) and (A2) into equations (3) and (7), the kinetic energy and potential energy for the j th element can be expressed, respectively, as

$$T_j = \frac{1}{2} \dot{q}_j^T [m_a] \dot{q}_j + [m_b] \dot{q}_j + Z_a, \quad (\text{A8})$$

$$U_j = \frac{1}{2} q_j^T [K_m] q_j - [K_g] q_j + \frac{1}{2} k \zeta^2, \quad (\text{A9})$$

where

$$\begin{aligned} [m_a] &= \rho A \int_0^{\ell_e} (\mathbf{H}_u^T \mathbf{H}_u + \mathbf{H}_v^T \mathbf{H}_v) dx \\ &+ \sum_{i=1}^n m_i (\mathbf{H}_u^T \mathbf{H}_u + \mathbf{H}_v^T \mathbf{H}_v) + M_G (\mathbf{H}_u^T \mathbf{H}_u + \mathbf{H}_v^T \mathbf{H}_v)_{x=\ell}, \end{aligned} \quad (\text{A10})$$

$$[m_b] = \rho A \int_0^{\ell_e} \mathbf{H}_v \dot{b} dx + \sum_{i=1}^n m_i \mathbf{H}_v \dot{b} + M_G (\mathbf{H}_v)_{x=\ell} (\dot{b} + \dot{\zeta}), \quad (\text{A11})$$

$$Z_a = \frac{1}{2} \left[\rho A \int_0^{\ell_e} (\dot{b})^2 dx + \sum_{i=1}^n m_i (\dot{b})^2 + M_G (\dot{b} + \dot{\zeta})^2 \right], \quad (\text{A12})$$

$$\begin{aligned} [K_m] &= \int_0^{\ell_e} \left\{ EA \left[\mathbf{H}_{u,x}^T \mathbf{H}_{u,x} + \frac{1}{4} v_x^2 \mathbf{H}_{v,x}^T \mathbf{H}_{v,x} + \frac{1}{2} v_x (\mathbf{H}_{u,x}^T \mathbf{H}_{v,x} + \mathbf{H}_{v,x}^T \mathbf{H}_{u,x}) \right] \right. \\ &\left. + EI [\mathbf{H}_{v,xx}^T \mathbf{H}_{v,xx}] \right\} dx, \end{aligned} \quad (\text{A13})$$

$$[K_g] = \int_0^{\ell_e} G(x) \mathbf{H}_{u,x} dx, \quad (\text{A14})$$

where the non-linear effect of the Euler-beam theory appears in the second term of the stiffness equation (A13). In this paper, the non-linear term is calculated at the previous time.

This is a simplified numerical technique [12] in the finite element method for the non-linear problem.

By assembling the equation of motion, we obtain the global ordinary differential equation

$$\mathbf{M}_1 \ddot{\mathbf{Q}}_1 + \mathbf{K}_1 \mathbf{Q}_1 = \mathbf{P}_1, \tag{A15}$$

where \mathbf{Q}_1 is the global displacement vector, \mathbf{M}_1 and \mathbf{K}_1 are the global mass and stiffness matrices respectively and \mathbf{P}_1 is the force vector. They are expressed as follows:

$$\mathbf{Q}_1 = [q_1 \ \cdots \ q_i \ \cdots \ q_{3n+1} \ \xi]^T_{1 \times (3n+1)},$$

$$\mathbf{M}_1 = \begin{bmatrix} & & 0 & & \\ & & \vdots & & \\ & \mathbf{M}_1^* & M_G & & \\ & & 0 & & \\ 0 & \cdots & M_G & 0 & M_G \end{bmatrix}_{(3n+1) \times (3n+1)}, \quad \mathbf{K}_1 = \begin{bmatrix} & & 0 & & \\ & & \vdots & & \\ & \mathbf{K}_1^* & & & \\ & & 0 & & \\ 0 & \cdots & 0 & 0 & k \end{bmatrix}_{(3n+1) \times (3n+1)},$$

$$\mathbf{P}_\ell = \left\{ \begin{array}{c} \mathbf{P}_1^* \\ -M_G \ddot{b} - \mu M_G \operatorname{sgn}(\dot{\xi}) \end{array} \right\}_{(3n+1) \times \ell}, \tag{A16-19}$$

where boundary conditions (14)–(16) are considered and

$$\mathbf{M}_1^* = \sum_{j=1}^{N_e} \left[\rho A \int_0^{\ell_e} (\mathbf{H}_{uj}^T \mathbf{H}_{uj} + \mathbf{H}_{vj}^T \mathbf{H}_{vj}) \, dx + \sum_{i=1}^n m_i (\mathbf{H}_u^T \mathbf{H}_u + \mathbf{H}_v^T \mathbf{H}_v) + M_G (\mathbf{H}_u^T \mathbf{H}_u + \mathbf{H}_v^T \mathbf{H}_v)_{x=\ell} \right], \tag{A20}$$

$$\mathbf{K}_1^* = \sum_{j=1}^{N_e} \left[\int_0^{\ell_e} \left\{ EA \left[\mathbf{H}_{uj,x}^T \mathbf{H}_{uj,x} + \frac{1}{4} v_x^2 \mathbf{H}_{vj,x}^T \mathbf{H}_{vj,x} + \frac{1}{2} v_x (\mathbf{H}_{uj,x}^T \mathbf{H}_{vj,x} + \mathbf{H}_{vj,x}^T \mathbf{H}_{uj,x}) \right] + EI [\mathbf{H}_{vj,x}^T \mathbf{H}_{vj,xx}] \right\} \, dx \right], \tag{A21}$$

$$\mathbf{P}_1^* = \sum_{j=1}^{N_e} \left[-\rho A \int_0^{\ell_e} \mathbf{H}_{vj} \ddot{b} \, dx - \sum_{i=1}^n m_i \mathbf{H}_v \ddot{b} - M_G \mathbf{H}_v \ddot{b} \Big|_{x=\ell} - \int_0^{\ell_e} G(x) H_{uj,x} \, dx \right]. \tag{A22}$$

A.2. THE SIMPLE-FLEXURE BEAM MODEL

Substituting equations (A1) and (A2) into equations (30) and (31) for the simple-flexure beam model, and following similar processes, one obtains

$$\mathbf{M}_2 \ddot{\mathbf{Q}}_2 + \mathbf{K}_2 \mathbf{Q}_2 = \mathbf{P}_2, \tag{A23}$$

where \mathbf{Q}_2 is the global displacement vector, \mathbf{M}_2 and \mathbf{K}_2 are the global mass and stiffness matrices respectively and \mathbf{P}_2 is the force vector. They are expressed as follows:

$$\mathbf{Q}_2 = [q_1 \ \cdots \ q_i \ \cdots \ q_{2n+1} \ \check{\xi}]_{1 \times (2n+1)}^T,$$

$$\mathbf{M}_2 = \begin{bmatrix} & & 0 \\ & & \vdots \\ & \mathbf{M}_2^* & M_G \\ & & 0 \\ 0 \ \cdots \ M_G \ 0 \ M_G \end{bmatrix}_{(2n+1) \times (2n+1)}, \quad \mathbf{K}_2 = \begin{bmatrix} & & 0 \\ & & \vdots \\ & \mathbf{K}_2^* & \\ & & 0 \\ 0 \ \cdots \ 0 \ 0 \ k \end{bmatrix}_{(2n+1) \times (2n+1)},$$

$$\mathbf{P}_2 = \left\{ \begin{array}{c} \mathbf{P}_2^* \\ -M_G \ddot{b} - \mu M_G \operatorname{sgn}(\dot{\check{\xi}}) \end{array} \right\}_{(2n+1) \times \ell}, \quad (\text{A24-27})$$

where

$$\mathbf{M}_2^* = \sum_{j=1}^{N_e} \left[\rho A \int_0^{\ell_e} (\mathbf{H}_{vj}^T \mathbf{H}_{vj}) dx + \sum_{i=1}^n m_i (\mathbf{H}_v^T \mathbf{H}_v) + M_G (\mathbf{H}_v^T \mathbf{H}_v)_{x=\ell} \right], \quad (\text{A28})$$

$$\mathbf{K}_2^* = \sum_{j=1}^{N_e} \int_0^{\ell_e} [EI (\mathbf{H}_{vj,xx}^T \mathbf{H}_{vj,xx} + G(x) \mathbf{H}_{vj,x}^T \mathbf{H}_{vj,x})] dx, \quad (\text{A29})$$

$$\mathbf{P}_2^* = \sum_{j=1}^{N_e} \left[-\rho A \int_0^{\ell_e} \mathbf{H}_{vj} \ddot{b} dx - \sum_{i=1}^n m_i \mathbf{H}_v \ddot{b} - M_G \mathbf{H}_v \ddot{b} \Big|_{x=\ell} \right]. \quad (\text{A30})$$

The force vector in the finite element formulation includes the acceleration of earthquake and the dry friction force.